Cold Air Activities in July 2004 and Its Impact on Intense Rainfalls over Southwest China*

CHEN Yan[1,2†](陈 艳) and DING Yihui[3](丁一汇)

1 *Laboratory for Climate Studies of China Meteorological Administration, National Climate Center, Beijing* 100081

2 *Yunnan Institute of Meteorological Sciences, Yunnan Meteorological Bureau, Kunming* 650034

3 *National Climate Center, Beijing* 100081

(Received May 28, 2007)

ABSTRACT

The severe rainfall events in the mid-summer of July 2004 and the roles of cold air in the formation of heavy precipitation are investigated by using daily observational precipitation data of China and NCEP/NCAR reanalysis. The results show that the severe rainfalls in Southwest China are closely related to the cold air activities from the mid-high latitudes, and the events take place under the cooperative effects of mid-high latitude circulation and low latitude synoptic regimes. It is the merging of a cold vortex over mid-latitudes with the northward landing typhoon and eastward Southwest China Vortex, as well as the abrupt transformation from a transversal trough into an upright one that causes three large alterations of mid-high atmospheric circulation respectively in the early and middle ten days of this month. Then, the amplitude of long waves soon magnifies, leading to the unusual intrusion of cold air to low-latitude areas in the mid-summer. Meanwhile, the warm and humid southwest summer monsoon is quite active. The strong interactions of cold air and summer monsoon over Southwest China result in the large-scale convective rainfalls on the southern side of cold air.

With regard to the activities of cold air, it can influence rainfalls in three prominent ways. Firstly, the incursion of upper-level cold air is often accompanied by partial southerly upper-level jet. The ascending branch of the corresponding secondary circulation, which is on the left front side of the jet center, provides the favorite dynamic upward motion for the rainfalls. Secondly, the southward movement of cold air contributes to the establishment of atmospheric baroclinic structure, which would lead to baroclinic disturbances. The atmospheric disturbances associated with the intrusion of cold air can destroy the potential instability stratification, release the convective available potential energy (CAPE) and finally cause convective activities. In addition, the advection processes of dry and cold air at the upper level along with the advection of humid and warm air at the lower level are rather significant for the reestablishment of potential instability in the precipitation area, which is one of the crucial factors contributing to persistent rainfalls.

Key words: cold air, Southwest China, strong rainfall, CAPE (convective available potential energy)

1. Introduction

The East Asian summer monsoon is directly influenced by the mid-high latitude circulation associated with the cold air activities, which is one of the main differences between the East Asian summer monsoon and the Indian summer monsoon (Zhang and Tao, 1998). Cold air has strong impacts on heavy rain processes in summer over North China. For instance, Ding et al. (1978) pointed out that the persistent advection of cold and dry air on the middle and upper levels as well as the low-level moist air provided favorable conditions for the reconstruction of the geopotential instability in the rainfall area, which was a significant factor for the rain to maintain, after they had studied the excessively torrential rain over Henan Province in mid-August 1975. In addition, the severe typhoon rainstorm during August 3–5, 1996 in Hebei Province resulted from the interaction between the southward dissipation of the cold air at the lower troposphere and the typhoon circulation. Accordingly, the simulation results suggested that the weak cold air intensified the shear and the upward motion in the lower atmosphere, providing the triggering and ascending condition for the rainfall. Meanwhile, the intrusion of weak cold air led to the accumulation

*Supported jointly by the National Natural Science Foundation of China under Grant No. 40675044, the National Key Development Program for Basic Research of China under Grant No. 2006CB400503 and the SCSMEX project.

†Corresponding author: chenyan@cma.gov.cn.

of water vapor carried by the partial southerly and southeasterly low-level jets, intensifying the moisture convergence.

Meiyu front, the primary rainfall system for East Asia in summer, belongs to the subtropical front combined with tropical monsoon and cold air from high-latitudes. Therefore, in the Meiyu season when there can be many intense rainstorms, the period of rainfall season and precipitation amount are determined not only by the position and intensity of mid-low latitude circulation regimes and water vapor transport, but also the situation of mid-high circulation (Zhang et al., 2002). Statistical results (Yao et al., 2005) show that when cold surge is strong, the Meiyu duration is long and the precipitation is plentiful, and vice versa. In addition, after summarizing rainstorm processes on the Meiyu front, Zhang and Tao (2004) pointed out that the third category of rainstorm forced by large-scale regimes was closely associated with cold air activities. Namely, the maintenance of the upper-level deep trough in the west of Meiyu front could lead cold air to rush southward frequently and converge with the warm and moist circulation which contains high instability energy, accompanying with the northward low-level jet in the troposphere. Thus, large-scale persistent rainstorm could occur in the front of the trough and even lead to severe disaster.

Moreover, the convergence of active summer monsoon and the southward cold air is one of the important reasons for the large-scale and strong rainfalls in South China. Although there was not the valley flood in China during July 2004, torrential rainstorms happened frequently in some regions and even brought about relatively severe rainstorms, floods, debris flow, and landslide, in Hunan, Hubei, Henan, and Yunnan Provinces, and Guangxi Region. Especially, the monthly precipitation is considerably above normal and the percentage of maximum precipitation anomaly exceeds 200% in the eastern Southwest China. Preliminary study presented that the troughs and ridges were prominent and the meridional circulation was strong in the high-latitude over Europe and Asia during that period, which contributed to the southward dispersion of cold air, and the large-scale rainstorms were closely related to it. It is well known that East Asia is controlled by the strong southwest monsoon and the warm and moist easterlies on the subtropical high southern fringe in mid-summer. As strong cold air intrudes southward to the low latitude area and interacts with the monsoon, it would cause large-scale intense rainfall. However, an interesting question comes out, how can the cold air rush down southward and reach very low latitudes and then affect the rainfall over Southwest China under the strong mid-summer monsoon situation. This paper studied the outbreaks of mid-summer cold air and its impacts on the rainfalls over Southwest China.

The datasets of July 2004 used in this paper include the daily precipitation of 668 meteorological stations, outgoing long-wave radiation (OLR) of the National Ocean and Air Administration (NOAA), and the reanalysis data of the National Center for Environmental Prediction and National Centers for Atmospheric Research (NCEP/NCAR), with a resolution of $2.5° \times 2.5°$.

2. Rainfall processes and large-scale circulation

The precipitation distribution of July 2004 in China resembles a belt in a direction of southwest-northeast (Fig.1), with the largest and the most intense rainfall region in Southwest China. And the

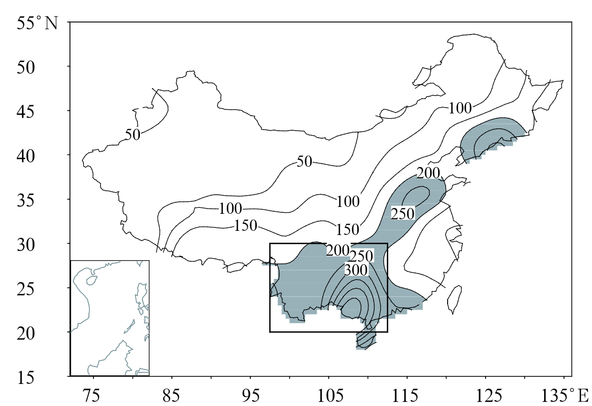

Fig.1. Monthly precipitation amounts over China in July 2004 (unit: mm). Shadings denote intense rainfall areas and the rectangle shows the area of Southwest China.

intense rainfall center, where the maximum precipitation exceeds 450 mm, is located in the east part of Southwest China. Hence, Southwest China refers to this intense rainfall area (20°-30°N, 97.5°-112.5°E) specifically in this paper, in which there are 138 meteorological stations. It can be seen from the temporal variations of the daily precipitation averaged over Southwest China (Fig.2), that there are sustaining rainfalls in July and exist 5 large-scale rainfall processes around July 5, 10, 14, 19, and 30. The five rainfall processes are identified according to the peak ratio of the rainfall station number to the total station number by the criterion of more than 70%, and they are called A, B, C, D, and E, respectively (Table 1). Obviously, the intensities of processes C and E are relatively weaker along with their shorter duration, compared with processes A, B, and C. The rainfall intensities of the latter three processes all exceed two standard deviations (13 mm) of the daily precipitation in this month. Particularly, the duration is more than 3 days for events B and D. Therefore, events A, B, and D are specified as Strong Rainfall Processes which will be investigated chiefly in the subsequent parts.

Table 1. Precipitation processes over Southwest China in July 2004

Title	Time period	Maximam daily precipitation (date)	Under influence of weather systems
A	July 5	18 mm (July 5)	ULT, SCV, LTS
B	July 8-11	21 mm (July 10)	ULT, NCV, SCV
C	July 14-15	10 mm (July 14)	ULT
D	July 18-22	23 mm (July 19)	ULT, SCV
E	July 30-31	12 mm (July 30)	ULT, ULCV

ULT: upper-level trough, SCV: Southwest China Vortex, LTS: landfalling tropical storm, NCV: Northeast cold vortex, and ULCV: upper-level cold vortex.

In the early July, there were two upper-level troughs located at the West Siberia to the east of Ural Mountains and the coastal area of East Asia, respectively, with a blocking high controlling the Baikal Lake and thereabouts. On July 4, the trough to the east of Ural Mountains deepened and moved southward, and then connected with the No. 0407 severe tropical storm Mindulle which landed on the coastal region of Zhejiang Province on July 3 and then moved northward. The trough over East Asian coast intensified rapidly, which caused the development of the high ridge around the Baikal Lake through downstream development. Meanwhile, it should be noticed that there was a low at 700 hPa over Southwest China (Fig.3a). On July 5, the tropical storm merged totally into the trough over the coast area of East Asia, and the eastward moving Southwest China Vortex also jointed it, which made the trough quite deep with its southern tip reaching around 20°N. Consequently, the cold air rushed southward over the most parts of China leading by the northwesterly in the west of the trough. Intense rainfall (process A) occurred in Southwest China. On July 6, the trough over the East Asian coast shrank northward (Fig.3c) and the rainfall process drew to an end.

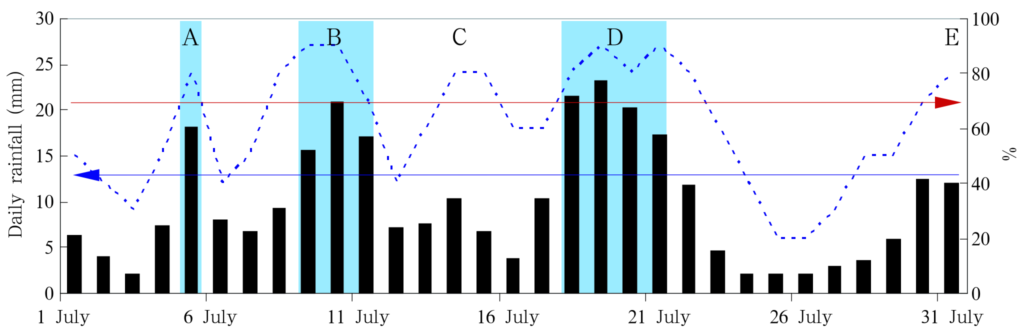

Fig.2. Time series of rainfall (black bar, unit: mm) averaged over Southwest China and the ratio of the stations where rainfall is observed (dotted line, unit: %). Shadings indicate the spans during which the daily precipitation exceeds 13 mm. Left and right arrows indicate the 13-mm precipitation and the ratio of 70%, respectively.

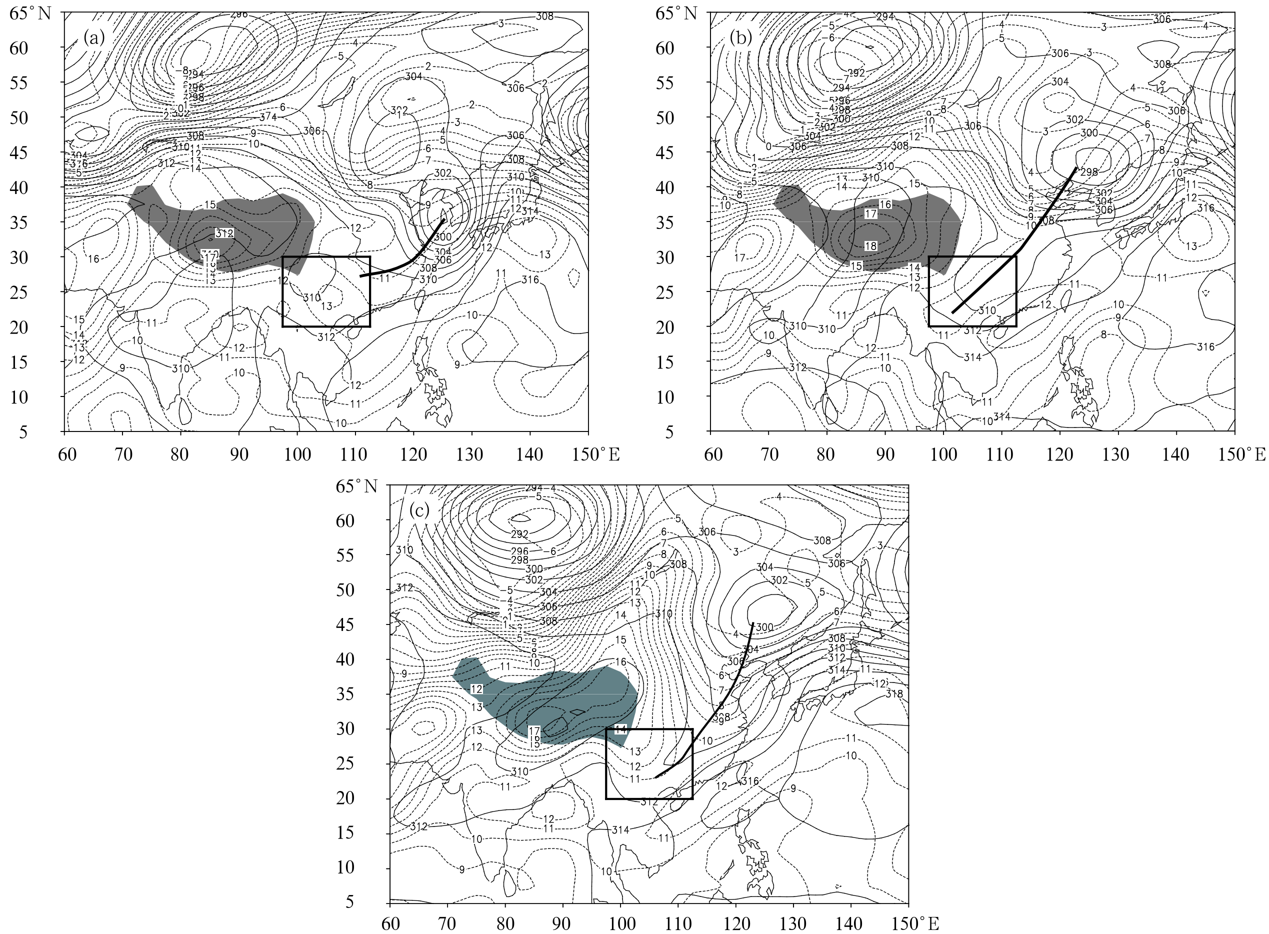

Fig.3. 700-hPa geopotential height (solid line, unit: dagpm) and temperature (dashed line, unit: °C) on (a) July 4, (b) July 5, and (c) July 6. The shadings indicate the plateau above 3000 m and the thick black line is the trough line.

On July 9, the high ridge, pointed from the Baikal Lake to Okhotsk Sea, strengthened and reached northeastward. Meanwhile, there existed a cold vortex over Northeast China and a low formed over Southwest China, with a weak high ridge between them (Fig.4a). On July 10 (Fig.4b), the high ridge over the Baikal Lake developed while the small high to the east of the Southwest China Vortex weakened and moved eastward so that the Southwest China Vortex connected with the northeast cold vortex, establishing a narrow low belt from Southwest to Northeast China. The cold air moved southward along the low belt and rainfall process B got strengthened.

The cold air activities associated with process D are caused by the trough transformation from transversal into upright (Fig.5). During July 13-15, there was warm advection to the west of the northeast-southwest high ridge which was located over the south Baikal Lake. The advection made the ridge keep intensifying as well as the northeasterly which led cold air to accumulate in the transversal trough and the trough to deepen. After July 16, the warm advection weakened, so did the high ridge. On July 17, a warm advection appeared over the rear part of the transversal trough, a noticeable cold advection to the east of it. It suggested that the trough would transform into upright. On July 18, the high ridge shrank southward rapidly and the trough transformed, cold air rushing down. On July 20, the weakened high ridge degenerated into a small east-moving high and then connected with the western. Therefore, the latter strengthened, while the small ridge was replaced by a low from the

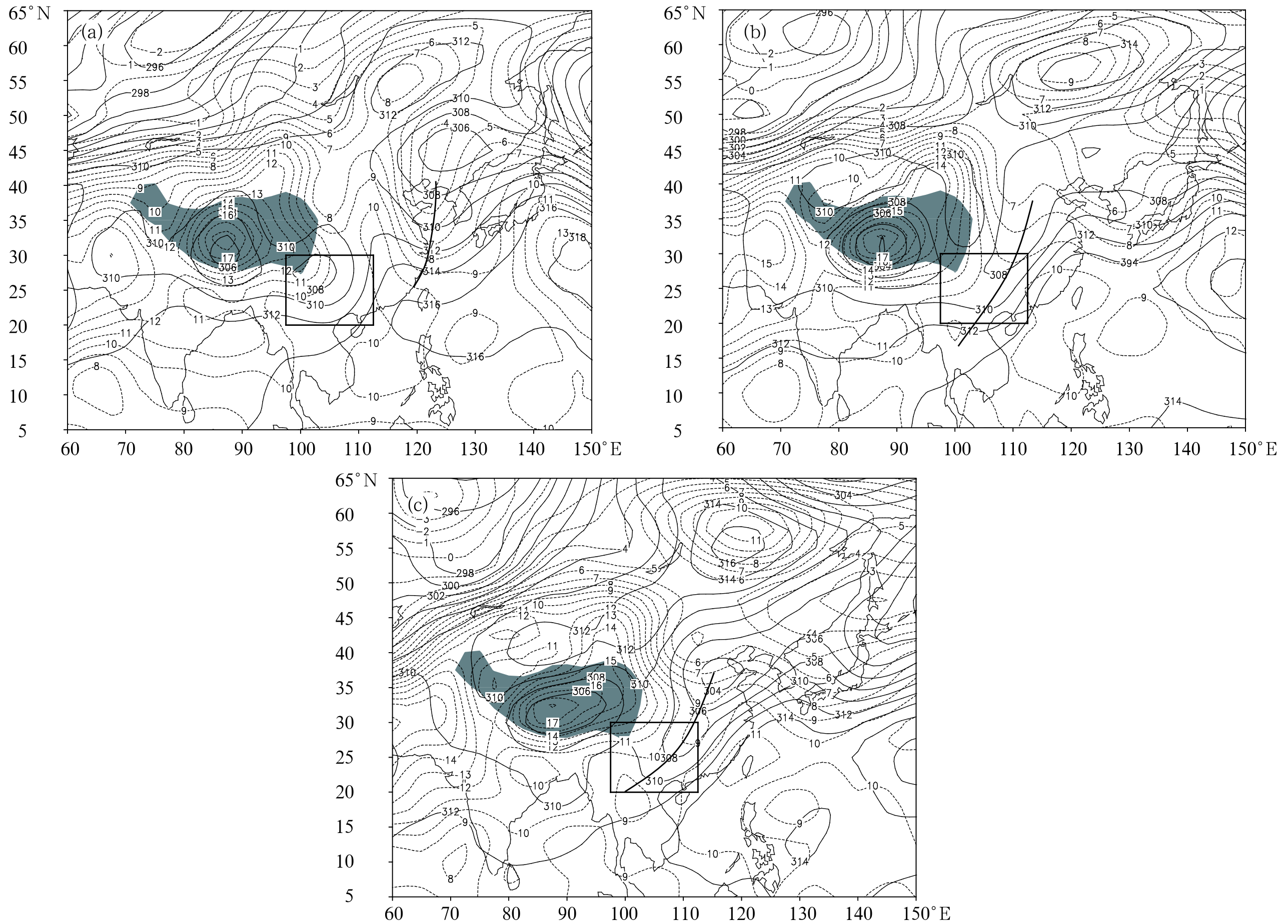

Fig.4. As in Fig.3, but for (a) July 9, (b) July 10, and (c) July 11.

west. A long-wave adjustment completed over East Asia. The isohypse was in north-south direction in the band of 50°-20°N to the east of 100°E, which made it possible for massive warm and humid air to surge northward. On July 21, the magnified subtropical high extended northwestward and Southwest China was covered by the partial easterly on the west fringe.

It can be seen from above analysis that those severe rainfall events happening in July over Southwest China are related to the cold air activities caused by the adjustment of the high-latitude circulation. However, it is rare for continuing large-scale cold air to move southward in the mid-summer.

3. Cold air activities and their roles in the rainfall processes

3.1 Cold air activities

The latent heating and condensation cooling caused by persistent precipitation would necessarily influence the structure of the atmospheric temperature, which might make it obscure for the temperature changes associated with the cold air activities. Therefore, for comparison, the temperature variations of the northern peripheral area (30°-35°N, 97.5°-112.5°E), where there was less rainfall, are also presented. It can be seen that from the time-height sections for the potential temperature anomalies over the northern peripheral area (Fig.6a) and Southwest China (Fig.6b), there are four conspicuous cooling events, corresponding to rainfall processes A-D, in the former area. The most remarkable negative anomalies (−4 K) of the temperature appeared at the mid-upper level of the troposphere during processes A and C. Compared with that of Southwest China (Fig.6b), only two noticeable negative anomaly centers emerged, indicating that two cold surges reached the quite low latitude and controlled this region. Moreover, the intense processes B

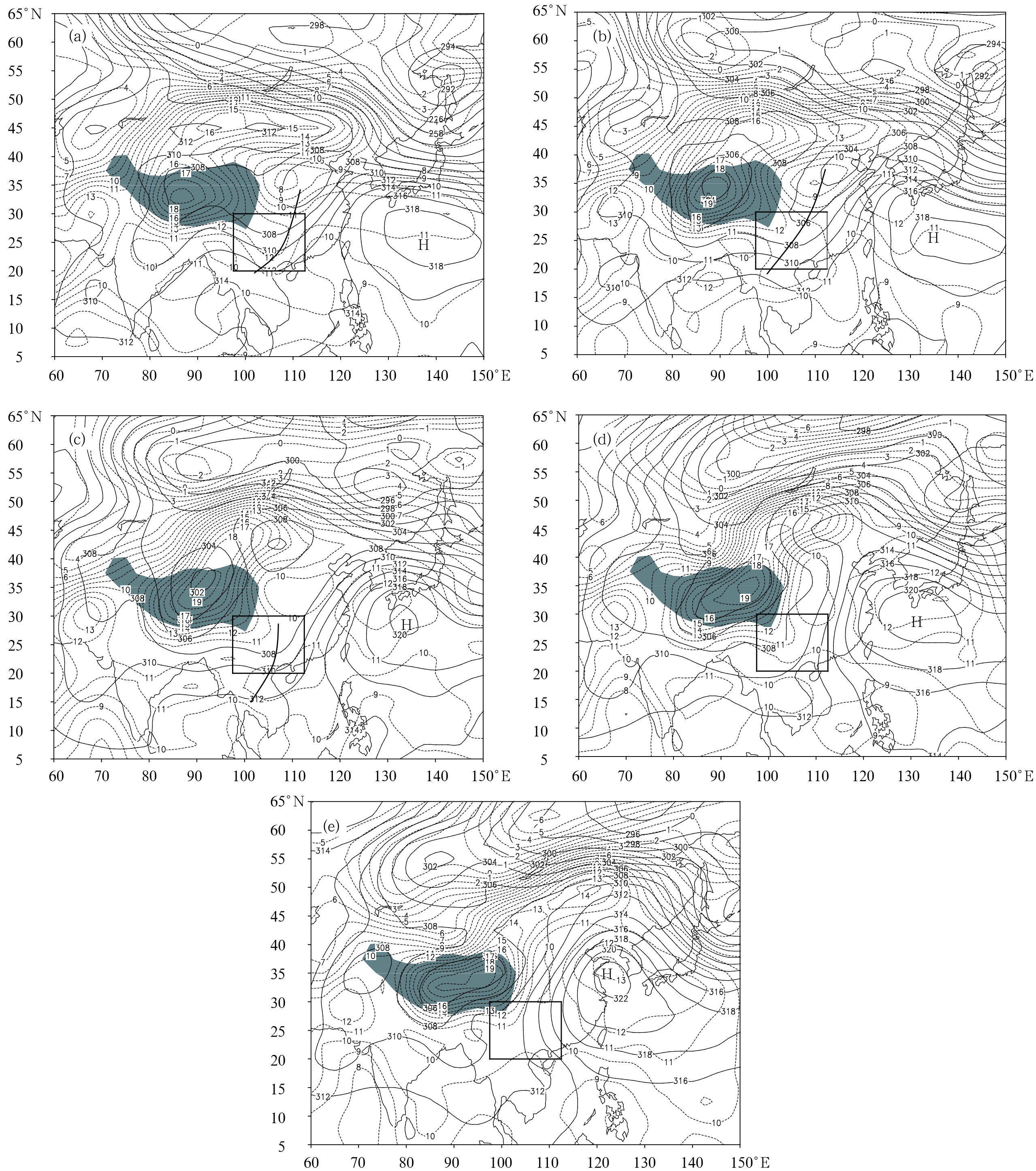

Fig.5. As in Fig.3, but for (a) July 17, (b) July 18, (c) July 19, (d) July 20, and (e) July 21.

and D were followed by two remarkable anomalies which were in the middle and upper atmosphere as well. This was the result of cold surges and condensation cooling of the precipitation. The first negative anomaly center manifested around July 7, and then followed substantial decrease of potential temperature at both upper and low levels. On July 10, the temperature dropped by 2 K at 150 hPa and more

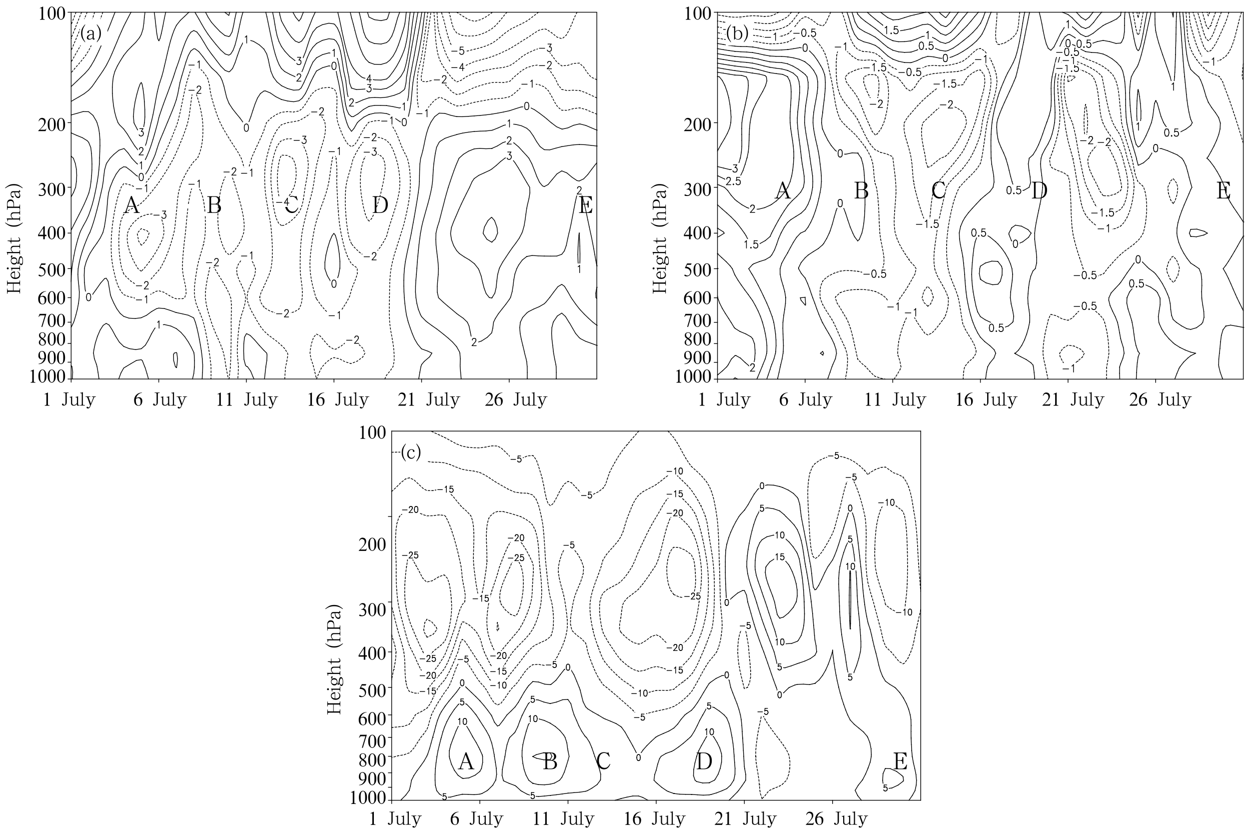

Fig.6. Time-height sections of the potential temperature anomalies (unit: K) in July 2004 averaged over (a) the northern border of Southwest China (30°-35°N, 97.5°-112.5°E), (b) Southwest China (20°-30°N, 97.5°-112.5°E), and (c) the section of relative vorticity of Southwest China (unit: 10^{-6} s^{-1}).

than −1 K at 600 hPa. Nevertheless, the decrease of temperature was not clear between them, which might be the result of latent heating caused by rainfall process B. After July 11, the temperature began to decrease rapidly in the whole troposphere till around July 16, marked the end of the first cooling process. The second remarkable cooling event took place after July 8, with the most strong temperature decrease of −2 K in the middle and upper levels of the troposphere. The changing magnitude was comparable to the first case. It drew to an end around July 25. From July 18 to 21, a relatively small variation of temperature in the middle troposphere was likely due to the latent heat released during process D. Obviously, these strong rainfall events were influenced substantially by the cold air in the middle and upper troposphere. Correspondingly, the variation of the mean relative vorticity of Southwest China (Fig.6c) presents that the change of upper level circulation played an important role in the precipitation processes. On the one hand, the vorticity in the lower troposphere was positive and in the upper negative during processes A-E. This could lead to convergence in the lower troposphere and divergence at the upper layer, and then contribute to upward motion. On the other hand, the variation of the negative vorticity in the upper troposphere was 1-3 days earlier than that of the positive in the lower layer, which also indicated that the variation of upper layer circulation played a significant role in the development of the lower layer system and those relevant intense rainfall events.

Furthermore, the time-latitude section of averaged 300-hPa heights and potential temperatures over 97.5°-112.5°E (Fig.7) shows that the four southward moving processes of systems were accompanied with cold air activities. Especially, the second and fourth

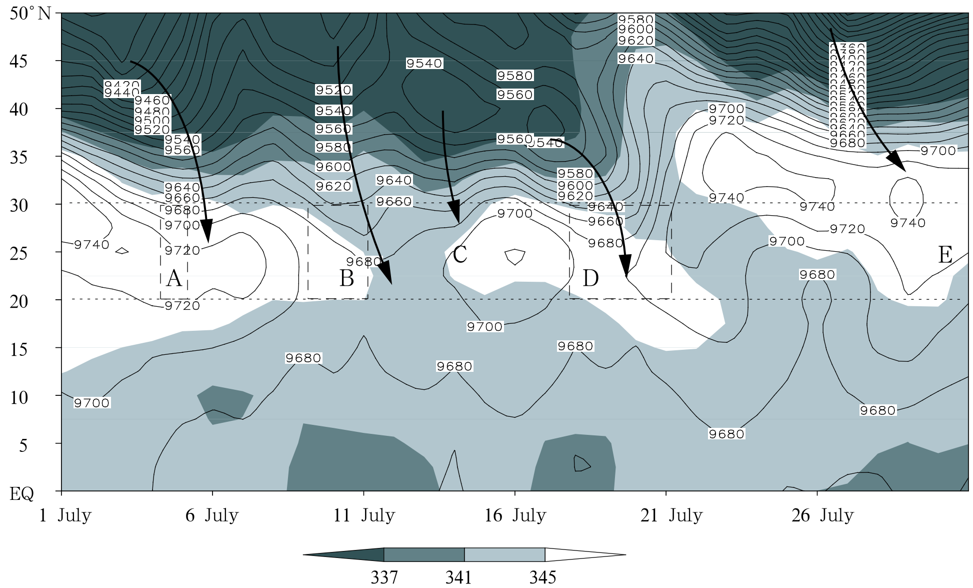

Fig.7. Time-latitude section of the 300-hPa height (solid line, units: gpm) and the potential temperature (shadings, units: K). The arrows indicate the moving trend of the upper level systems.

processes manifested by the potential temperature were rather remarkable with the most southern tips reaching around 20°N. This was the main reason for the substantial decrease of the temperature over Southwest China after rainfall events B and D, which is consistent with the previous analysis. In the last ten days of July, the systems at mid-high latitudes were relatively stable and the southward intrusion of cold air was weaker than before.

According to the previous analysis, although the variation of the temperature and height fields can expose to some extent the activities of mid-high systems, it cannot identify every case of cold surge and the associated precipitation process. It is well known that the potential vorticity of dry air is conservative under adiabatic and frictionless conditions. Since the humidity content of the cold air over mid-high latitudes is relatively small, the heat exchange between the air mass and the environment can be neglected with regard to short process. Therefore, it is conservative and can be used as the indicator of cold air activities (Hoskins et al., 1985; Shuts, 1983; Lu et al., 1994; Wang et al., 1996).

In the p-coordinate system, if the horizontal change of ω is neglected, the dry potential vorticity PV can be written as:

$$PV \approx -g(\zeta + f)\frac{\partial \theta}{\partial p} + g\Big(\frac{\partial v}{\partial p}\frac{\partial \theta}{\partial x} - \frac{\partial u}{\partial p}\frac{\partial \theta}{\partial y}\Big), \qquad (1)$$

where ζ is the vertical vorticity, f is the Coriolis parameter, and the other symbols are common meteorological symbols.

In order to investigate the change of potential vorticity, the time-latitude section of averaged 300-hPa potential vorticity over 97.5°-112.5°E (Fig.8a) was plotted. Continual outbreaks of the high potential vorticity centers from the mid-high latitude are noticeable, reflecting the southward transportation of cold air. The cold air reached 30°N and even further in four cases. The first case took place in the early July, with the strong cold air moving southward from the mid-high latitude and reached about 22°N. The second occurred in the late of the first decade and the early of the second decade of July, with the lowest latitude near 20°N. Then, the third event outbroke in the middle of July, with the cold air starting to move around 40°N, while the potential vorticity was small to the north of 40°N. According to the previous analysis, it was the result of the development of high blocking in the mid-high latitude and the continuous accumulation of cold air in the transversal trough to its south. Moreover, it is clear that the duration of cold air moving southward was relatively long with the cold air lingering around 27°N. It did not move southward until the third decade of July, with the most southern fringe about 20°N and even further, and the region between 20° and 30°N was almost covered by cold air then. The fourth cold surge happened in the late of this month, but it was relatively weak. To investigate the time-altitude section of averaged potential vorticity over Southwest China, Fig.8b presents that the potential vorticity was increasing with altitude and there were six centers appearing between 500 and 300 hPa. The first, second, fourth, and sixth centers were stronger than the other two with a tendency stretching to the ground, and the time they happened was right consistent with rainfall processes A-E. These characteristics demonstrate that potential vorticity can clearly depict moving southward cold air from the mid-high latitude and its stretching downward associated with those rainfall events occurring in Southwest China.

3.2 Cold air disturbance to the atmosphere

Vigorous cold air can not only change the thermal structure of the atmosphere but also the dynamic structure in a considerable degree. Concerning the variation of potential vorticity, it is conservative along the air parcel trajectory in the inviscid and adiabatic barotropic atmosphere. Therefore, each of the southward moving center of potential vorticity at the upper level was accompanied by the advection of positive vorticity (figure omitted). Nevertheless, it was the strong upward motion in the front of the southward moving cold air that had directly impacted the rainfall, which could strengthen the upward motion when the strong cold air got closed to Southwest China. From the time-altitude section of averaged vertical velocity over Southwest China (Fig.9), the upward motion was rather conspicuous in the whole month, especially in the early and middle July. There was robust upward motion in the span of rainfall processes except for the weak case C. Prominently, it was the most vigorous and deepest during case D along with the longest duration. Then, there was no evident upward motion from July 23 to 26 and less precipitation was observed. Furthermore, it was relatively weak during case E.

First of all, the robust upward motion identified above may be closely related to the upper-level jet. From the climatological point of view, after the onset of the summer monsoon, the dominant feature over Southwest China is the switch of upper-level wind from westerly to easterly until the retreat of summer monsoon (Chen et al., 2006). However, from the variation of the wind in July of Southwest China (Fig.10a), the 200-hPa easterly turned into northwest wind around July and it did not recover until July 20. During this period, there were four noticeable acceleration motions of the west wind component which were exactly coincident with rainfall processes A-D. In fact, the wind switch and acceleration reflect the southward moving of the westerly jet on the northern flange of the South Asian high, showing the intimate relationship between the southward moving jet and the robust rainfall events. Thereby, it is presented in Fig.11 about the 200-hPa horizontal wind field and vertical velocity field on July 10 and 19 when the most strong precipitation was observed during rainfall processes B and D. Noticeably, there were strong partial southerly centers to the west or southwest of the southward moving cold air, with the maximum wind velocity over 30 m s^{-1}. Due to the extreme nonhomogeneity of the wind velocity, secondary circulations that were orthogonal to the jet could be triggered, based on the dynamic equations, around the entrance and exit areas of the jet respectively (Ding, 2004). Obviously, in these two cases, Southwest China was right situated at the ascending branch area that was in the left front of the upper-level jet. The secondary circulation moved southward with the jet center along with its ascending branch, providing rather favorable dynamical lifting conditions.

On the other hand, the outbreak of cold air can have the vertical disturbances of the atmosphere developed through increasing the barocinity. Take process B for example, on the figure of latitude-altitude sections of the pseudo-equivalent potential temperature and specific humidity along 107.5°E (Fig.12), $\theta_{\rm se}$ was high in the band of 20°-30°N in which heavy rainfalls took place. The θ_{se} isopleth stretched downward like a funnel and it was small at the middle and upper levels on the south and north of it, suggesting there was relatively cold and dry air there. In other words, a band lined with dense θ_{se} isopleth was over the south

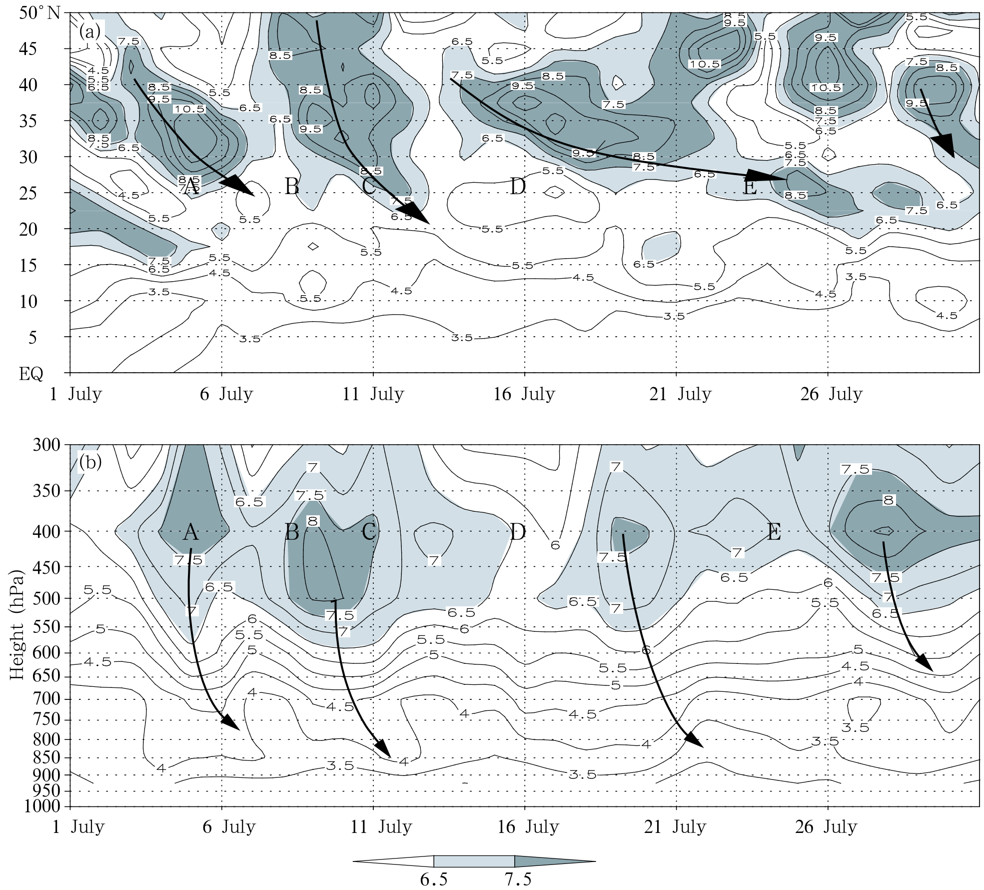

Fig.8. (a) The time-latitude section of 300-hPa potential vorticity (unit: 10^{-7} m^2 s^{-1} K kg^{-1}, designated as PVU in the following parts for short) with the data averaged over the longitude bands between 97.5° and 112.5°E, and (b) the time-altitude section of averaged potential vorticity of Southwest China. The arrows indicate the moving trend of the potential vorticity center.

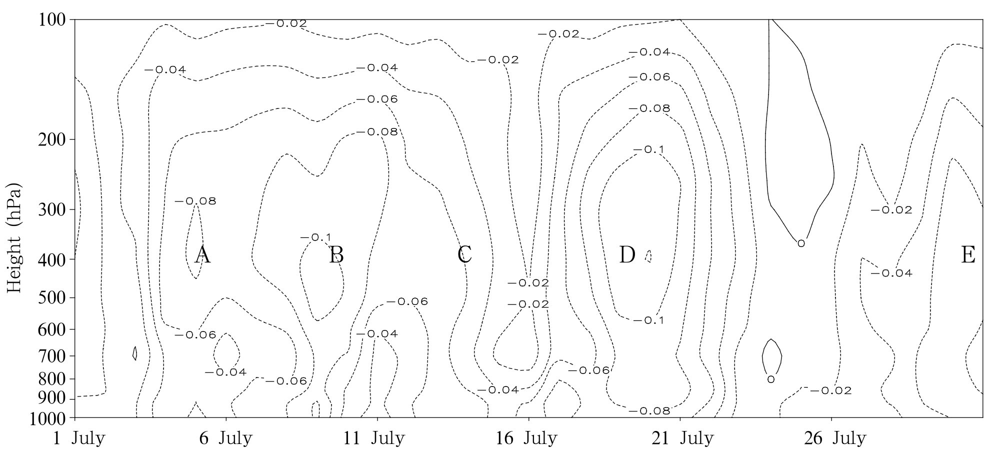

Fig.9. The time-altitude section of vertical velocity (unit: Pa s^{-1}) averaged over Southwest China.

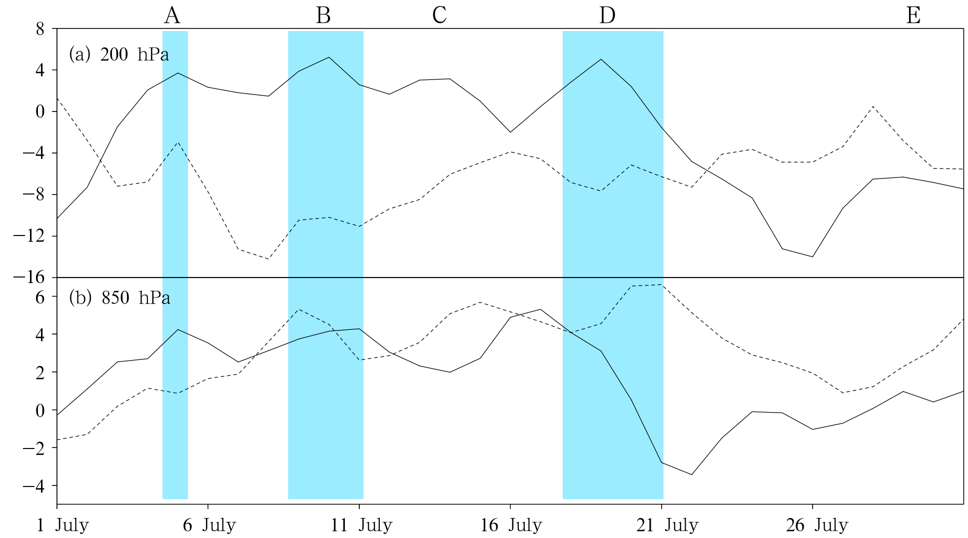

Fig.10. The evolution of (a) 200-hPa and (b) 850-hPa wind speed (unit: m s^{-1}) averaged over Southwest China. The solid line denotes zonal wind and dotted the meridional wind. Shadings indicate the spans of intense rainfalls.

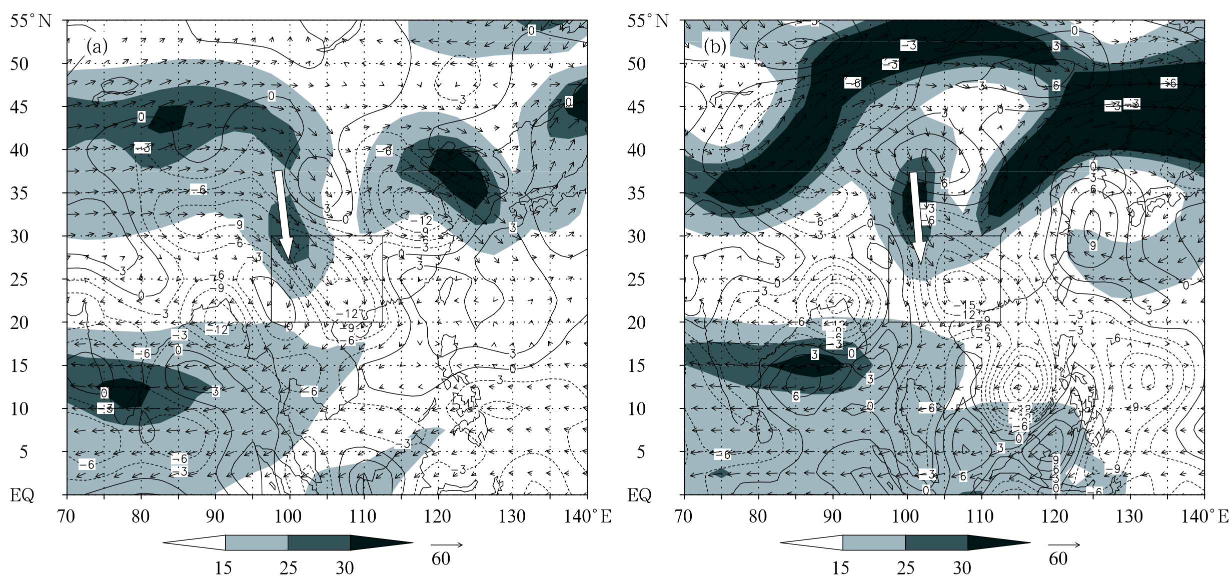

Fig.11. 200-hPa wind field (unit: m s^{-1}) and vertical velocity ω (unit: 0.01×Pa s^{-1}) on (a) July 10 and (b) July 19. Shadings denote the areas where the wind speed exceeds 15 m s^{-1}.

and north of Southwest China, which was the typical structure of storm. Particularly, the isopleth of θ_{se} to the north was very steep, where was the key area for the development of strong vertical vorticity (Wu et al., 1995). With the southward advance of the cold air, the compact band of θ_{se} and strong upward motion moved down. As the intense cold air was at the middle and upper levels of the troposphere, the isopleth of θ_{se} clearly tended to tilt southward when moving forward on July 11, so did the upward vertical motion. Hereafter, the precipitation abated in Southwest China.

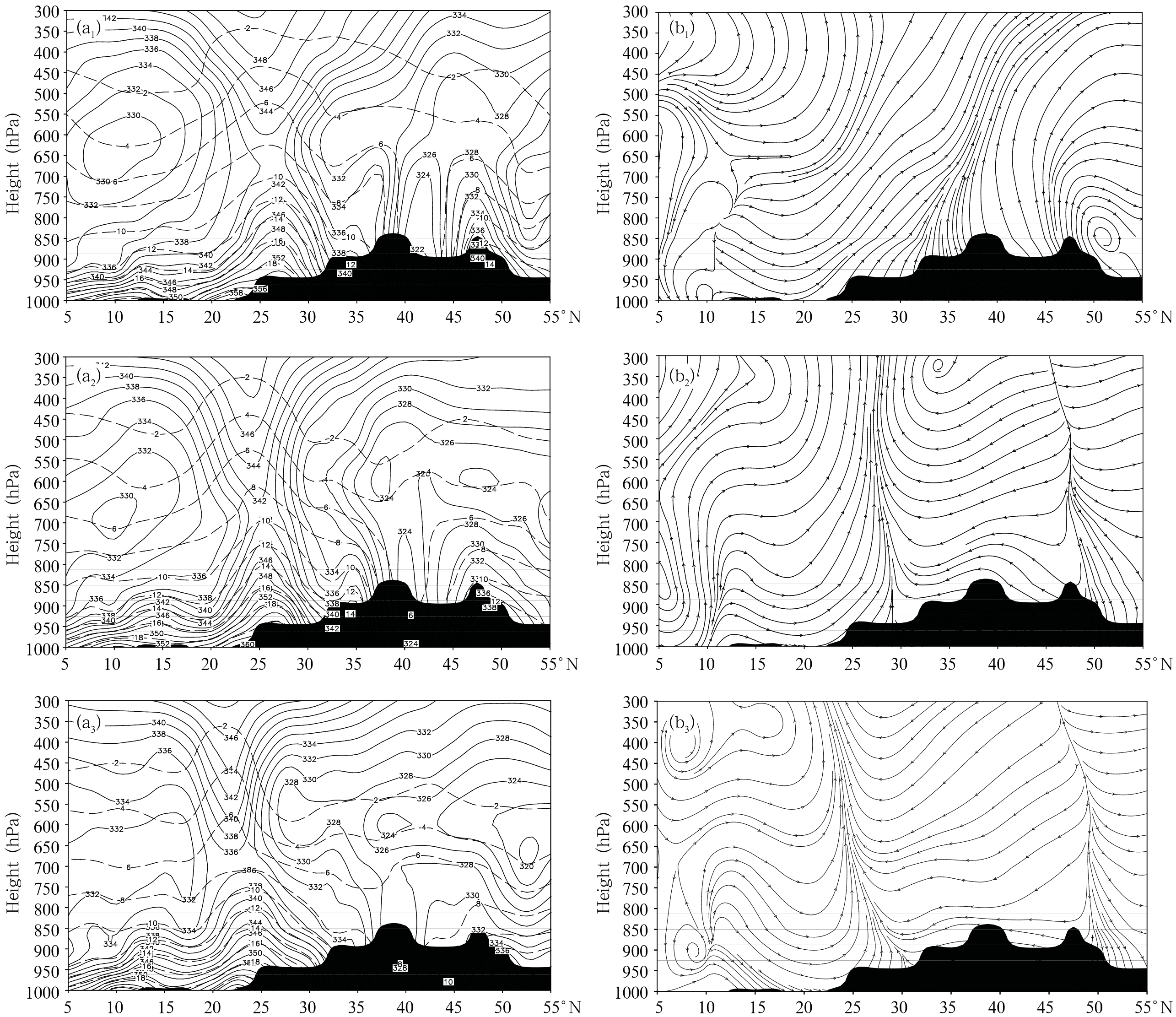

Fig.12. Daily latitude-altitude section of pseudo-equivalent potential temperature θ_{se} (solid line, unit: K) and specific humidity (dashed line, unit: g kg^{-1}) across 107.5°E on (a$_1$) July 9, (a$_2$) July 10, and (a$_3$) July 11. And (b$_1$)-(b$_3$) present the corresponding meridional circulation, in which ω is magnified by 50 times.

3.3 The cold air activities and the development of convection

The characteristics of precipitation can be identified through calculating the apparent heat source Q_1 and moisture sink Q_2. If their heights of the peak value on each vertical profile are near, then the heating is mainly caused by frontal or persistent rainfall, otherwise the heating is primarily associated to convection precipitation. In order to examine the calculating accuracy and find out the principal heating term, the horizontal distribution of vertical integration of Q_1 and Q_2 is given in Fig.13. As for process D, the centers of Q_1 and Q_2 were in the same order located in Southwest China on July 19, which was coincident with the distribution of precipitation. This demonstrates that the calculation is accurate and the heating in Southwest China is primarily the result of latent heating released by condensation. The characteristics of other rainfall events in this month are alike.

Figure 14 depicts the vertical profiles of apparent heat source Q_1 and apparent moist sink Q_2 as well as

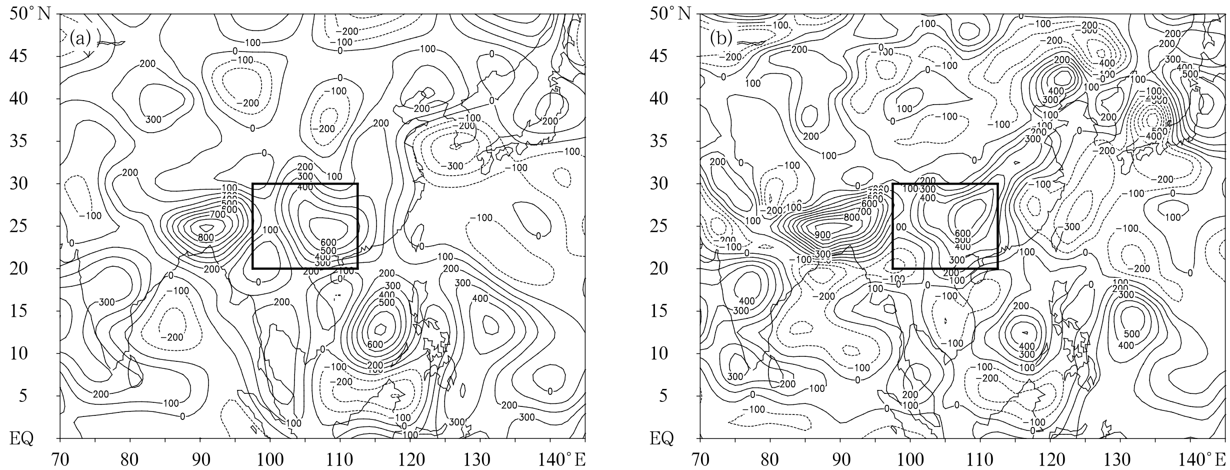

Fig.13. The vertical integrated (a) apparent heat source Q_1 (unit: W m^{-2}) and (b) apparent moist sink Q_2 (unit: W m^{-2}) on July 19.

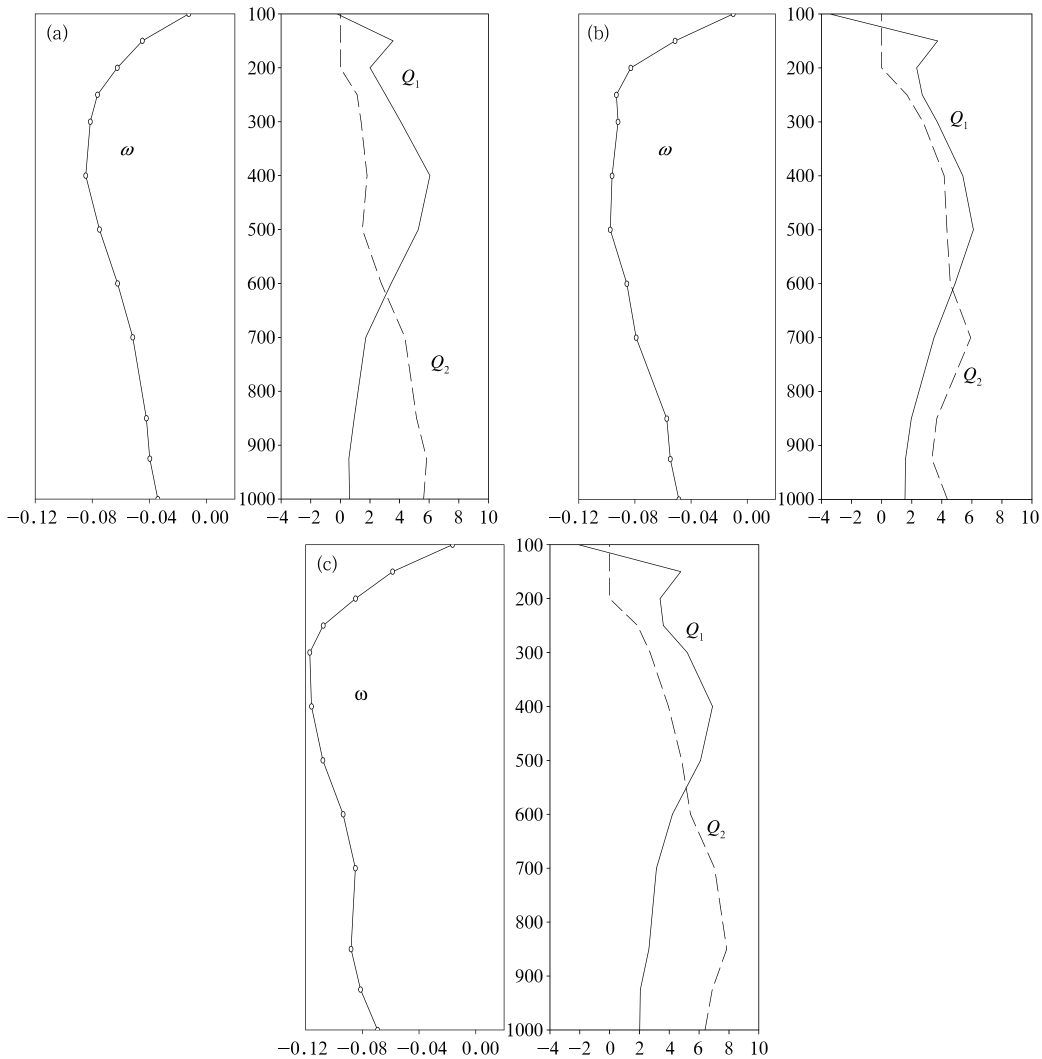

Fig.14. Profiles of apparent heat source Q_1 (K day^{-1}), apparent moist sink Q_2 (K day^{-1}), and vertical velocity ω (Pa s^{-1}) on (a) July 5, (b) July 10, and (c) July 19.

the vertical velocity on July 5, 10, and 19. It is clear that the upward motion was robust during the rainfall processes, especially on July 19, with the most magnificent value between 500 and 200 hPa. Through comparing the vertical distribution of Q_1 and Q_2, there existed a secondary peak in 200-100 hPa besides the most remarkable one at 400 hPa and thereabouts, excluding the one on July 10, in which the biggest value of Q_1 was at 500 hPa. Unlike the distribution of Q_1, the peak value of Q_2 was under 800 hPa on July 5 and 19, and it was around 700 hPa on July 10. In other words, the convective vertical transport was significant in rainfall processes A and D, and the release of latent heat was closely related to the convective activities, indicating the convective characteristics of the precipitation. With regard to case B, the vertical eddy transport was relatively weak despite convective precipitation.

Based on the foregoing analysis, it can be concluded that the vertical perturbation induced by the southward moving cold air is the major reason that brought about the release of convective instability energy and the convection. From the variation of vertical distribution of $\theta_{\rm se}$ over Southwest China (Fig.15), there brought about obvious low value ($\theta_{\rm se}$ <336 K) in the middle and upper levels of the troposphere before each rainfall process, suggesting it was dry in this layer and extremely unstable under 600 hPa ($\frac{\partial\theta_{\rm se}}{\partial z} < 0$), which provided a favorable stratification condition for the subsequent convection. With the increase of cold air or the high positive potential vorticity, the vertical transport of heat and water vapor intensely developed, convective instability disappeared, severe rainfall processes began and it had been tending to be neutral instability. After the rainfall process finished, the convective instability could establish again by advections of cold and dry air at the middle and upper layers and the moist and instable air in the low layer. However, the convective instability had not been established before the fifth increase of the upper-level potential vorticity occurred due to lack of water vapor transport at that time, there was no distinct precipitation during that period. It can be seen that the destruction of convective instability and the occurrence of precipitation were tightly related to the intrusion of upper-level cold air.

In fact, the development of convection also depends on the instability energy when the atmosphere is under instability conditions. The instability energy can be estimated by calculating the convective available potential energy (CAPE). Figure 16 is the temporal evolution of averaged CAPE over Southwest China.

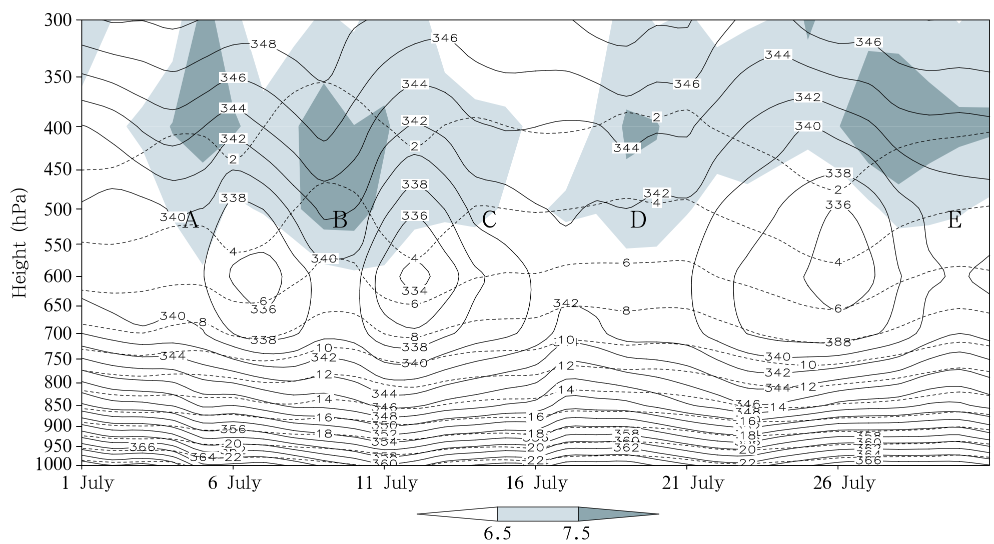

Fig.15. Latitude-time section of pseudo-equivalent potential temperature $\theta_{\rm se}$ (solid line, unit: K) and specific humidity (dotted line, unit: g kg^{-1}) averaged over Southwest China. Shadings indicate the potential vorticity center.

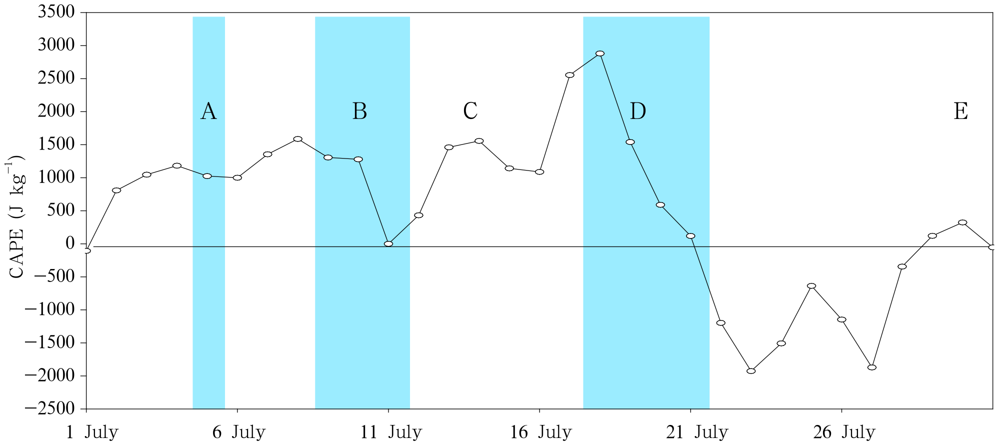

Fig.16. Evolution of CAPE (unit: J kg^{-1}) averaged over Southwest China. Shadings indicate the spans of intense rainfall.

Obviously, CAPE was positive in the middle and late decades of July, which was very favorable for the development of convection. In addition, it was strong up to 3000 J kg^{-1} before process D, which was the direct cause for intense convective precipitation. Nevertheless, with the intrusion of cold air, CAPE was released and diminished so as to develope convective activities. In the last ten days of this month, CAPE became negative and it did not develope until the end of this month.

In order to investigate the cold air activities and the variation of CAPE, daily composites of cases A, B, and C are presented along with the 300-hPa potential vorticity (Fig.17). Clearly, CAPE had increased two days before the strongest rainfall day over the eastern part of Southwest China with the biggest value exceeding 3500 J kg^{-1}. One day before (−1 day), it kept increasing in this region and extending northeastward. Meanwhile, the cold air represented by the center of positive potential vorticity began to move southward. On the very rainy day (0 day), the cold surge rushed southward and wedged in the north part of Southwest China and the CAPE began to decrease. On the next day (1 day), the cold air continued to move forward and the CAPE was almost released thoroughly, and rainfall abating. Two days later (2 days), the cold air pulled back and rainfall process finished. In other words, the heavy rainfalls might happen when the robust vertical turbulence induced by cold air activities moved to a certain region where it was in an extremely convective instable condition and there was sufficient moisture transport.

4. Discussions and conclusions

Due to lack of large terrain barrier in the Asian summer monsoon area, cold air from the mid-high latitudes can penetrate to low latitudes and influence the weather and climate there directly. This paper largely explored the cold air activities and their impacts on the rainfall events in the mid-summer through studying three strong rainfall processes happening in July 2004 over Southwest China.

The study shows that those three torrential rainfall events happening in the early and middle of July over Southwest China are caused by the cooperative effects of mid-high latitude circulation and low latitude synoptic regimes. Namely, it is the merging of cold vortex over mid-latitudes with the northward landing typhoon and eastward Southwest China Vortex, as well as the abrupt transformation from transversal into upright trough that lead to three large alterations of mid-high atmospheric circulation respectively. Then, the amplitude of long waves soon magnifies, bringing about the unusual intrusion of cold air to the low latitude areas in the mid-summer. Meanwhile, the warm and humid southwest summer monsoon is quite active. The strong interactions of cold air and summer monsoon over Southwest China result in the large-scale convective rainfalls on the southern side of cold air. With the southward moving of the cold air, the precipitation area extends southward. With regard to the activities of cold air, it can influence rainfalls through three prominent ways. Firstly, the incursion of upper-level cold air is often accompanied by partial southerly upper level jet. The ascending branch of the

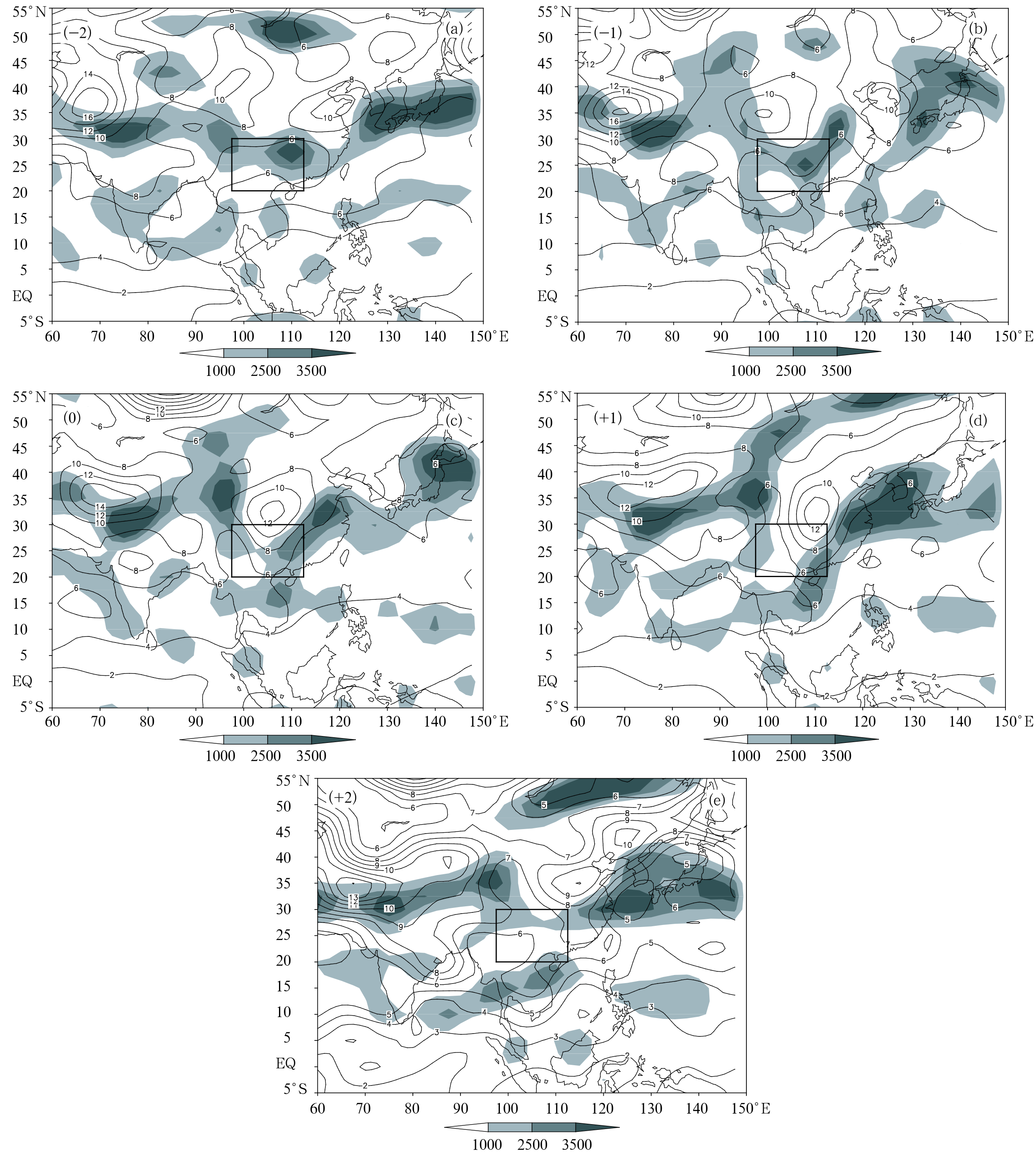

Fig.17. Daily evolution of composite CAPE (unit: J kg^{-1}, shadings denote the CAPE greater than 1000) and 300-hPa potential vorticity (solid line, unit: PUV), by centering the strongest rainfall days (denoted by 0) of the three intense rainfall events A, B, and D.

corresponding secondary circulation, which is on the left front side of the jet center, provides the favorite dynamic upward motion for the rainfalls. Secondly, the southward movement of cold air contributes to the establishment of atmospheric baroclinic structure, which could lead to baroclinic disturbances. The atmospheric disturbances associated with the intrusion of cold air can destroy the potential instability stratification, release the convective available potential energy, and finally cause convective activities. In addition, the advection processes of dry and cold air at the upper level along with the advection of humid and warm air at the lower troposphere are rather significant for the reestablishment of potential instability in the precipitation area, which is one of the crucial factors contributing to persistent rainfalls.

Although this paper focuses on the impact of cold air activities at mid-upper level of troposphere on the rainfall events, the activities and variation of low-latitude and low-level systems also play important roles in those processes. From Fig.10 it can be seen that it was generally controlled by southerly at 850 hPa in the first and middle ten days of July during which intense rainfall happened. Moreover, there even emerged southwest monsoon surges before the rainfall events or during the rainfall processes. After July 20, the southwesterly turned into southeasterly because of the intensification and extending westward of the West Pacific subtropical high. Compared with the variation of 200-hPa wind field (Fig.11a), the vertical shear was rather clear in Southwest China during the intense rainfall processes. Each rainfall event was accompanied not only by the increase of upper-level northwesterly but also the lower-level partial southerly. Robust wind shear was favorable for the maintenance and development of convective systems, while the strengthening of lower-level partial southerly was helpful for the transport of warm and humid air to Southwest

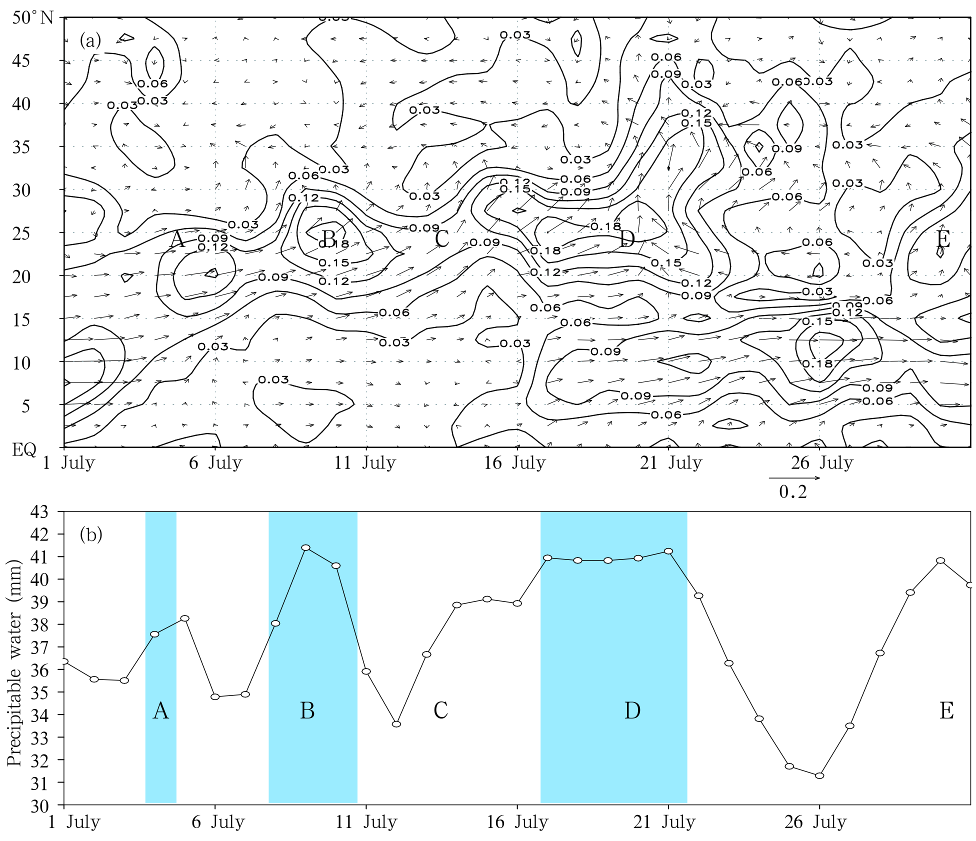

Fig.18. (a) The averaged time-latitude section (97.5°-112.5°E) of the 850-hPa water vapor transport (units: kg m^{-1} s^{-1} hPa^{-1}) and (b) the variation of precipitable water (unit: mm) over Southwest China. Shadings indicate the spans of intense rainfall.

China. From the variation of averaged 850-hPa water vapor transport over 97.5°-112.5°E, three spans of intense water vapor transport in 20°-30°N emerged, which correspond to rainfall processes A, B, and D. In the middle ten days of July, the southwestward water vapor transport was dominant. After July 20, it turned into southeast transport as the result of atmospheric circulation adjustment. However, no matter southwesterly or southeasterly, persistent water vapor transport brought sufficient moisture for Southwest China, which increased the precipitable water (Fig.18) and provided necessary moist conditions for the torrential rainfalls.

Acknowledgements. The authors would like to thank Dr. Liu Yanju and Dr. Li Qiaoping for their support throughout this study.

REFERENCES

Chen Yan, Ding Yihui, Xiao Ziniu, et al., 2006: The impact of water vapor transport on the summer monsoon onset and abnormal rainfall over Yunnan Province in May. *Chinese Journal of Atmospheric Sciences*, **30**(1), 25-37. (in Chinese)

Cui Xun, 2004: Onset of rainy season over North China and drought over the Yangtze-Huaihe Valley associated with Meiyu ending−monthly weather review of July 2004. *Meteorological Monthly*, **30**(10), 58-61. (in Chinese)

Ding Yihui, Cai Zeyi, and Li Jishun, 1978: Study on the excessively torrential rain over Henan in the middle of August 1975. *Scientia Atmospherica Sinica*, **2**(4), 276-289. (in Chinese)

Ding Yihui, 2005: *Advanced Synoptic Meteorology.* China Meteorological Press, Beijing, 138-149.

Hoskins, B. J., M. E. Mclntyre, and A. W. Robertson, 1985: On the use and significance of isentropic potential vorticity maps. *Quart. J. Roy. Meteor. Soc.*, **111**, 877-946.

Lu Er, Ding Yihui, and Li Yuehong, 1994: Isentropic potential vorticity analysis and cold air activity during the period of excessively heavy rain over Changjiang-Huaihe River basin in 1991. *Quarterly Journal of Applied Meteorology*, **5**(3), 266-274. (in Chinese)

Luo H., and M. Yanai, 1994: The large-scale circulation and heat sources over the Tibetan Plateau and surrounding areas during the early summer of 1979. Part II: Heat and moisture budgets. *Mon. Wea. Rev.*, **112**, 966-989.

Ma Lan, Wu Xiaojing, Jiang Jixi, et al., 2003: Analysis of characteristics of summer monsoon and heavy rainfall over South China in 2001. *Journal of Applied Meteorological Science,* **14**(4), 445-451. (in Chinese)

Shuts, G. J., 1983: The propagation of eddies in diffluent jet streams eddy vorticity forcing of blocking flow fields. *Quart. J. Roy. Meteor. Soc.*, **109**, 737-761.

Tan Zhinian, Huang Xuesong, and He Hui, 2004: Analyses of the cause of abnormal large amounts of rain in July of 2004. *Journal of Guangxi Meteorology*, **25**(4), 11-14. (in Chinese)

Wang Jianzhong, Ma Shufen, and Ding Yihui, 1996: Application of potential vorticity theory to analysis the formation mechanism of torrential rain. *Quarterly Journal of Applied Meteorology*, **7**(1), 19-27. (in Chinese)

Wu Guoxiong, Cai Yaping, and Tang Xiaojing, 1995: Moist potential vorticity and slantwise vorticity development. *Acta Meteor. Sinica*, **53**(4), 387-405. (in Chinese)

Xu Guoqiang and Hu Xin, 1999: The weak cold air influence upon heavy rain in August 1996 and its simulation. *Meteorological Monthly*, **25**(7), 17-20. (in Chinese)

Yao Yeqing, Wang Xingrong, and Mu Xianjun, 2005: Relationships between Meiyu and cold air. *Meteorological Monthly*, **31**(5), 77-79. (in Chinese)

Yu Yubin and Yao Xiuping, 2000: The diagnosis analysis of potential vorticity for a severe typhoon rainstorm in North China. *Plateau Meteorology*, **19**(1), 111-120. (in Chinese)

Yuan Jiashuang and Shou Shaowen, 2001: Potential vorticity analysis in cold air activities during the South China torrential rain in 1998. *Journal of Nanjing Institute of Meteorology*, **24**(1), 92-98. (in Chinese)

Zhang Qingyun and Tao Shiyan, 1998: Influence of Asian mid-high latitude circulation on East Asian summer rainfall. *Acta Meteor. Sinica*, **56**(2), 199-211. (in Chinese)

Zhang Shunli, Tao Shiyan, Zhang Qingyun, et al., 2002: Large and meso-α scale characteristics of intense rainfall in the mid- and lower reaches of the Yangtze River. *Chinese Science Bulletin*, **47**(6), 467-473.

Zhang Xiaoling and Tao Shiyan, 2004: Three types of heavy rainstorms associated with the Meiyu front. *Chinese Journal of Atmospheric Sciences*, **28**(2), 187-205. (in Chinese)